

Materials Advances

Accepted Manuscript

This article can be cited before page numbers have been issued, to do this please use: S. Khaleel, C. Lacroix, D. R. Hall, M. Cavarroc, D. Menard and C. Santato, *Mater. Adv.*, 2026, DOI: 10.1039/D6MA00204H.



This is an Accepted Manuscript, which has been through the Royal Society of Chemistry peer review process and has been accepted for publication.

Accepted Manuscripts are published online shortly after acceptance, before technical editing, formatting and proof reading. Using this free service, authors can make their results available to the community, in citable form, before we publish the edited article. We will replace this Accepted Manuscript with the edited and formatted Advance Article as soon as it is available.

You can find more information about Accepted Manuscripts in the [Information for Authors](#).

Please note that technical editing may introduce minor changes to the text and/or graphics, which may alter content. The journal's standard [Terms & Conditions](#) and the [Ethical guidelines](#) still apply. In no event shall the Royal Society of Chemistry be held responsible for any errors or omissions in this Accepted Manuscript or any consequences arising from the use of any information it contains.

Spin Dynamics and Magnetization in Sepia Melanin by Electron Paramagnetic Resonance and Vibrating Sample Magnetometry

Shahid Khaleel^a, Christian Lacroix^a, Darren Hall^a, Marjorie Cavarroc^b, David Ménard^a, Clara Santato^a

*a: Department of Engineering Physics, Polytechnique Montreal
2500 Ch. de Polytechnique, Montréal, QC H3T 1J4*

b: Safran Tech, Materials and Processes Department, 78114 Magny-Les-Hameaux, France

Corresponding authors: clara.santato@polymtl.ca
david.menard@polymtl.ca
c.lacroix@polymtl.ca

Abstract

Sepia melanin, a eumelanin member of the melanin biopigment family, is part of the dark Sepia ink liberated by cuttlefish for defence and camouflage. It takes its name from Sepia Officinalis, a common species of cuttlefish from where Sepia melanin is extracted. Sepia melanin contains stable radicals i.e. carbon centered radicals (CCR) and semiquinone radicals (SQR), making it a promising candidate for organic spintronic and bioelectronic applications. The behavior of the radicals is strongly influenced by hydration, as water molecules interact with redox-active sites and modulate charge and spin configuration. In this study, we investigate the magnetic behavior of Sepia melanin in both dry and hydrated states using Electron Paramagnetic Resonance (EPR) spectroscopy in ambient conditions and Vibrating Sample Magnetometry (VSM) across a temperature range of 150-360 K. EPR analysis revealed a decrease in signal intensity, a slight increase in g-value and an increase in transverse relaxation time upon hydration, in agreement with literature. VSM measurements suggested weak ferromagnetism in both states, with saturation magnetization (M_s) and remanent magnetization (M_r) decreasing upon hydration. As expected, this ferromagnetic behavior weakens with increasing temperature. Despite this decline, ferromagnetic behavior persists above 360 K. To discard the presence of metallic chemical elements possibly contributing to the magnetic behavior, we conducted an Instrumental Neutron Activation Analysis



(INAA) study. In addition, we probed the surface elemental composition by X-ray Photoelectron Spectroscopy (XPS). While INAA revealed trace concentrations of Fe, Cu, Ni, and Co in the bulk, the presence of such elements was below the detection limit of XPS. These findings suggest that the observed magnetism could arise predominantly from the organic radical matrix, particularly CCR and SQR, rather than contributions from metals.

Introduction

The magnetic properties of organic materials have garnered increasing attention for applications in organic spintronics, bioelectronics, and biomedical devices.¹⁻³ Organic materials are technologically relevant for their mechanical flexibility, low processing temperatures, lightweight, and biocompatibility.⁴⁻⁶

Research efforts have focused on achieving ferromagnetism in organic materials through the presence of radical species (unpaired electrons)^{7, 8}. In 1963, McConnell⁹ proposed that aromatic and olefinic molecular structures featuring free radicals could π - π stack in a crystalline lattice, enabling ferromagnetic exchange interactions between the spins of π -electrons by promoting parallel spin alignment in adjacent molecules. However, it was not until 1991 that the first metal-free organic ferromagnet was identified, i.e. p-nitrophenyl nitronyl nitroxide crystal, where the interaction between radicals in neighboring molecules leads to spin alignment.¹⁰ More recently, compounds like tetracyanoquinodimethane (TCNQ) have demonstrated weak ferromagnetism even at room temperature (saturation magnetization $\sim 10^{-3}$ emu/g), further highlighting the viability of radical-based magnetic order in organic systems.¹¹

Among organic materials, eumelanin, the black-brown biopigment of the melanin family, stands out as a promising candidate for exhibiting magnetic behavior because of its *intrinsic* radicals and



quinone-based redox properties.¹²⁻¹⁴ Further, eumelanin has been extensively investigated for its moisture-dependent electrical response, broad optical absorption and metal-binding affinity.¹⁵⁻¹⁸

Eumelanin results from the oxidative polymerization of two building blocks (monomers) namely 5,6-dihydroxyindole (DHI) and 5,6-dihydroxyindole-2-carboxylic acid (DHICA). DHI and DHICA possess multiple sites for polymerization, which causes them to form different oligomers, of different sizes. These oligomers undergo hierarchical self-assembly via $\pi - \pi$ stacking, resulting in protomolecules composed of approximately 4–5 stacked layers, with an interlayer spacing of around 3.5 Å and a lateral size around 20 Å^{16, 19, 20}. These protomolecules further forms about 10 to 15 nm-sized structures through a combination of $\pi - \pi$ interactions and edge-to-edge hydrogen bonding. These same forces also drive the formation of larger spherical granules ranging between 100 and 300 nm in diameter.¹⁶ High-resolution atomic force microscopy has shown that these granules exhibit small protrusions with average widths of ~19 nm and heights of ~3 nm.²⁰

Due to the incomplete polymerization of the monomers (DHI and DHICA), the material features carbon-centered free radicals that remain unpaired.^{13, 21, 22}

Sepia melanin, a natural form of eumelanin, is extracted from the ink sac of *Sepia Officinalis* (a common form of cuttlefish). Sepia melanin exists in different redox forms. These include the reduced hydroquinone (HQ), intermediate semiquinone (SQ), and oxidized quinone (Q) forms along with Q tautomeric form, quinone imine (QI). The comproportionation equilibrium regulating the concentration of HQ, SQ and Q in wet environments, shifts toward the formation of SQ and protons with the increase of water concentration. Charge transport is mediated by hopping of electrons between trap states. Protons act as mobile charge carriers, contributing to Sepia melanin's electrical response.^{16, 17, 19, 20, 23, 24}



The magnetic properties of melanin have traditionally been associated with its stable unpaired electrons, attributed to SQR and CCR.^{12-14, 21, 25-27} These radicals not only define melanin's paramagnetic character but also play a key role in its electrical response. However, the nature and origin of this magnetic response, whether attributable to the *polymer* backbone i.e. due the radicals present in the melanin, or emergent from environmental interactions (e.g., hydration, metals present because of the synthesis in an open, living environment), remain under investigation.

Electron Paramagnetic Resonance (EPR) spectroscopy has been pivotal in elucidating the radical-based nature of melanin and the role of radicals in explaining its electrical response. Studies consistently report the presence of intrinsic, stable semiquinone-type, free radicals across various types of melanin (i.e. black soldier fly eumelanin²⁸, bovine eye eumelanin²⁹, dopa eumelanin³⁰, human hair eumelanin³¹ etc.), manifested as a dominant narrow signal in EPR spectra.¹⁴ Hydration-dependent EPR studies have shown that water significantly alters the radical signal's linewidth and g-value, indicating that water changes the local electronic environment of the radicals.^{13, 14} The radicals present in melanin are not only structural markers but also active participants in charge transport via hopping, thereby linking melanin's paramagnetic character with its transport behavior.^{25, 32} Furthermore, chemical modifications, such as sulfonation of melanin, affect spin concentration and g-values, suggesting tunability of melanin's radical properties through functionalization. In sulfonated melanin, the addition of an electron to the neutral molecule can cause the release of a $-\text{SO}_2\text{CH}_3$ group attached to a quinone oxygen, with the spin localizing on the $-\text{SO}_2\text{CH}_3$ radical. This suggests that higher g-values may be associated with trapped sulfonated groups originating from S-melanin.^{26, 27}

Vibrating sample magnetometry (VSM) is a powerful technique to characterize the magnetic properties of materials by detecting changes in its magnetization within a uniform magnetic field



with different intensities.^{33, 34} Previous studies on melanin using (VSM) have identified weak ferromagnetism in natural melanin, copper-doped melanin, and melanin-ZnO composites, with the magnetic response decreasing at elevated temperatures³⁵. However, these studies did not fully explore or explain the origin of weak ferromagnetism in undoped, natural melanin.^{35, 36}

To evaluate the potential of eumelanin for radical-based technologies and devices, it is essential to deepen our understanding of its spin-related properties, particularly in natural form such as Sepia melanin. This investigation should account for the material's hierarchical structure.²⁰ Additionally, the elemental composition of Sepia melanin, including the presence of metals such as iron, copper, and zinc etc., may play a role in influencing its magnetic and electronic behavior.^{32, 37}

In this study, we investigate the magnetic properties of Sepia melanin in both dry and hydrated states using EPR spectroscopy and VSM. EPR measurements were performed to probe changes in unpaired electron populations and their local environment upon hydration. VSM was employed to examine how hydration affects the magnetization behavior and temperature-dependent magnetic responses.

The aim of this work is to investigate how hydration affects the macroscopic magnetic response. Our working hypothesis is that hydration not only modifies the relative concentration of radical species (CCR and SQR) as already reported in the literature but also alter spin-spin interactions in Sepia melanin. By combining EPR spectroscopy, which probes radical spin dynamics, with VSM measurements, which probe macroscopic magnetization, we aim to establish a relationship between microscopic radical behavior and macroscopic magnetic ordering. In contrast to previous investigations of eumelanin magnetism, this work provides new insight by revealing how hydration affects both the EPR signatures and the static magnetization curves of biosourced Sepia melanin.



Materials and Methods

Materials for the treatment of edible cuttlefish ink

Cuttlefish ink (Stareef Seafood Boston, sourced from Spain) was purchased at a fish market in Montreal. Hydrochloric acid (HCl, ACS reagent grade, 37%) was purchased from Acros Organics. Monobasic and dibasic sodium phosphate solutions (0.5 M in water), along with ethanol (ACS reagent, 99.8%), ethyl acetate, 1-propanol ($\geq 99.5\%$), and 1-methoxy-2-propanol ($\geq 99.5\%$) were purchased from Sigma-Aldrich.

Treatment of edible cuttlefish ink and sample preparation

Sepia melanin powder was obtained from the commercial cuttlefish ink using a method modified from previously documented procedures.^{17, 32, 38} In brief, 300 g of commercial cuttlefish ink were dispersed in 500 mL of 2M hydrochloric acid and stirred continuously for 24 hours at ambient temperature. The resulting mixture was subjected to centrifugation (Allegra-X30R Centrifuge, Beckman Coulter), followed by sequential treatment steps: three washes with 0.5 M HCl, and one wash each with deionized (DI) water, a phosphate buffer (comprising 0.02% vol/vol monobasic sodium phosphate 200 mM, 32.49% vol/vol dibasic sodium phosphate 200 mM, and 67.49% DI water), ethanol, DI water again, and ethyl acetate. The final stage involved four additional rinses with DI water. All centrifugation steps were performed at 10,000 rpm and 5 °C, with durations of 15 minutes for the HCl solutions, ethanol, and ethyl acetate, and 25 minutes for the DI water and buffer steps. The so obtained material was then lyophilized at $-80\text{ }^{\circ}\text{C}$ for 3 days to remove excess water, resulting in a dry, fine black Sepia melanin powder. This protocol typically leads to 30–35 g of melanin from 300 g of raw ink, i.e. a yield of about 10–12% by weight.

The Sepia melanin powder was stored under two different conditions for at least 24 hours: in a nitrogen glovebox (H_2O and $\text{O}_2 < 5\text{ ppm}$) for dry samples, and in a humidity chamber with relative



humidity exceeding 90% for hydrated samples. A humidifier filled with deionized (DI) water was used to maintain the high-humidity environment in a Cole-Parmer Mini Humidity Chamber (model 03323–14). A fan was employed to ventilate the chamber and ensure uniform moisture distribution. We tracked the variations in relative humidity (RH) using two instruments: a USB portable hygrometer (REED R6020 Datalogger) and a microcontroller-based sensor (ETS 5100). Prior to weighing, Sepia melanin powder was ground to eliminate large agglomerates. Sample masses were measured using an analytical balance with a precision of 10^{-5} g. For hydration studies, the sample was first weighed before hydration, placed in the humidity chamber, and then weighed again after 24 hours of exposure. The weight percentage gain due to hydration was calculated using the following equation:

$$\%wt = \frac{W_2 - W_1}{W_1} \times 100$$

where W_1 and W_2 are the weight of the sample before and after hydration. The weight percentage gain after hydration was approximately 15%. To prepare the pellets, each sample (~300 mg) was weighed using an analytical balance. The measured powder was then compressed into disc-shaped pellets using a Carver Laboratory Press (Model C) under a pressure of 10 metric tons for 60 seconds by means of a manual hydraulic press machine (Specac's Atlas Series) and the resulting pellets were about 1 mm-thick.

Electron Paramagnetic Resonance (EPR) Spectroscopy

An EPR spectrum is obtained by keeping the radiation frequency (ν) constant while varying the magnetic field (B). Absorption (or resonance) takes place when the magnetic field tunes the energy difference (ΔE) between the two spin states to match the energy of the electromagnetic radiation.

This resonance condition is expressed as:

$$\Delta E = h\nu = g\mu_B B_0 \quad (1)$$



Where

$$g = \frac{h\nu}{\mu_B B_0} \quad (2)$$

h is Planck's constant (6.626×10^{-34} Js), ν is the microwave frequency (GHz), μ_B is the Bohr magneton (9.274×10^{-24} J/T) and B_0 is the resonance field (T).

EPR measurements were performed on Sepia melanin using a Bruker Magnettech ESR5000 spectrometer. The spectra were recorded at room temperature with a magnetic field ranging from 313 mT to 363 mT, corresponding to a total sweep width of 50 mT. The sweep time was set to 60 seconds. A microwave power of 10 mW was used, with a modulation amplitude of 0.2 mT. The frequency of the resonant cavity was 9.447 GHz. Dry and hydrated samples (i.e. S_epr_dry and S_epr_wet) of Sepia melanin in the form of powder was used for EPR measurements. The Sepia melanin powder was dried for ~2 days in glovebox and hydrated for ~1 day in hydration chamber (RH~95%) before EPR measurements.

Vibrating Sample Magnetometry (VSM)

Magnetization measurements of Sepia melanin samples were carried out using an EV9 VSM system from ADE Technologies, varying both the magnetic field strength and temperature. In short, the vibration of the sample induces an alternating magnetic signal, which is picked up by detection coils and converted into a voltage proportional to the sample's magnetization, allowing precise characterization of its magnetic behavior.

Measurements of the temperature dependence of magnetization across a temperature range of 150–360 K at a step of 70 K were performed. For varying the temperature, the sample is placed in an oven tube equipped with a thermocouple in which circulates N₂ gas. A heating element located in the oven tube allows to precisely control the temperature of the N₂ gas using a PID loop. For



temperature measurements below room temperature, the N₂ gas was pre-cooled using liquid N₂ before entering the oven tube.

For the magnetization measurements, the Sepia melanin pellet was cut into small pieces of almost square shape with a mass of ~50 mg. Before the measurement on Sepia melanin sample, a calibration using disc made of nickel with a known magnetic moment was used. Then, the Sepia melanin sample was glued at the end of the sample holder (Pyrex rod) using a double-sided tape. The M-H loops at each temperature were obtained. Then, the sample was removed from the sample holder, and the signal of the sample holder (without the sample) was measured at each temperature again. The signals of the sample holder could then be subtracted from the first set of measurements to obtain the signal from sample only.

Instrumental Neutron Activation Analysis (INAA)

The Instrumental Neutron Activation Analysis (INAA) elemental characterization of the Sepia melanin was performed using Polytechnique Montréal's SLOWPOKE-2 nuclear reactor. This analysis technique uses neutron sources to activate radioisotopes and in turn determine elemental concentrations through the analysis of gamma-ray spectra. The reactor has a maximum thermal output of 20 kW and uses High-Assay Low-Enriched Uranium (HALEU) as its fuel source. Triplicates of the sample with masses of approximately 1 g were prepared in 1.6 mL high-purity polyethylene vials and injected into one of the reactor's irradiation sites with a thermal neutron flux of roughly 5×10^{11} neutrons/cm²/s. The samples were irradiated for 30 s and then 5 hours in order to adequately activate the radionuclides of interest (short- and long-lived, respectively). Once irradiated, the radioactive samples were counted on a high-purity germanium (HPGe) detector to collect the gamma-ray spectra at different decay times. The mass concentrations were then determined using Polytechnique Montréal's specialized INAA software, and the analysis was conducted for a variety of elements (see Table 3).



X-ray Photoelectron Spectroscopy (XPS)

XPS analysis was performed using a Thermo Scientific ESCALAB 250Xi spectrometer equipped with a monochromatic Al K α X-ray source (photon energy = 1486.68 eV). The X-ray source operated at a power of 218.8 W (14.7 kV, 14.9 mA), with the base pressure in the analysis chamber maintained at 1.0×10^{-8} Torr. Measurements were carried out over an analyzed surface area of approximately 1000 μm in diameter, with an electron take-off angle of 0° , providing a probing depth of less than 10 nm. Survey spectra were recorded using a pass energy of 150 eV and an energy step size of 1.0 eV. Background subtraction was performed using the Smart method, and quantification was based on the Thermo Al sensitivity factor table. All binding energies were charge-corrected with reference to the C 1s peak at 284.8 eV. Powdered samples were pressed onto conductive copper tape and mounted on a glass substrate for analysis.

Result and Discussion

EPR Analysis

EPR spectra of dry and wet samples of Sepia melanin show that the intensity of EPR signals of wet samples decreases as compared to the dry samples (Fig. 1).

EPR signals are believed to arise from two radical species i.e. CCR and SQR.^{13, 25} Mostert et al proposed that with hydration, the concentration of CCRs decreases and that of the SQRs increases, with an overall decrease of the EPR signal.¹³ In dry melanin, CCR are stabilized within stacked oligomeric sheets. Upon hydration, SQR units are formed, contributing an extra electron to the aromatic system. This alters the distribution of negative charge across the atoms in the molecule. As a result, the π - π stacking between oligomeric sheets is disrupted, leading to the de-stacking of oligomers, as explained by Hunter and Sanders.³⁹ This exposes the CCR to the aqueous environment and reduces the EPR signal intensity.^{13, 40} Therefore, the reduced EPR intensity in hydrated sample of Sepia melanin could be attributed to a combined effect of CCR depletion, spin



delocalization within enhanced conductive pathways, and increased spin–lattice relaxation¹², all of which modify the EPR spectrum.

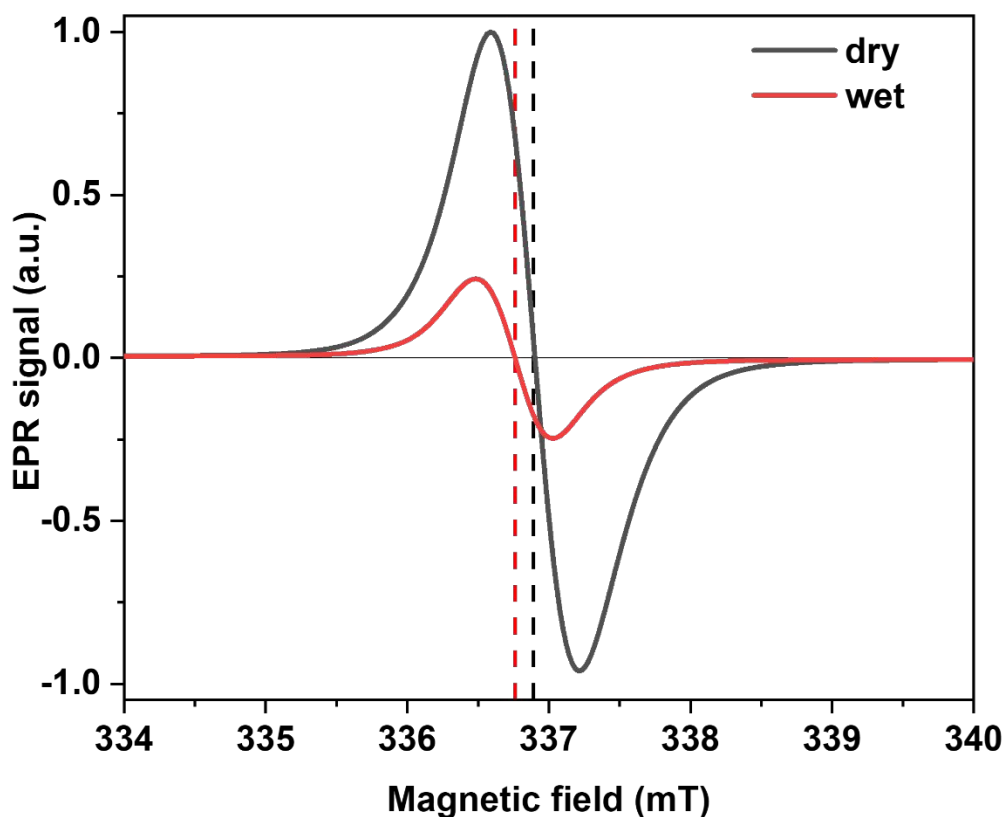
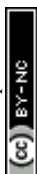


Fig. 1: X-band EPR spectra of dry (black solid line, $S_{\text{epr_dry}}$) and wet (red solid line, $S_{\text{epr_wet}}$) samples of *Sepia melanin*.

We have calculated the g -value using Eq. 2 for dry and wet samples (see *Materials and Methods*) to be 2.0034 and 2.0043, respectively. The line width decreases upon hydration (see Table 1), along with a concomitant reduction in EPR signals.^{13, 26} EPR measurements show a decrease in signal intensity, a slight shift in the g -value and an increase of transverse relaxation time (see Table 1 of main file and Calculation S1 in Supplementary Information) upon hydration, indicating changes in the local electronic environment and in the interactions between radicals. As reported



previously in the literature, the changes in EPR spectra possibly originates from transformations of CCR and SQR.¹³

Table 1: Comparison of g-value, linewidth, resonance field and the relaxation time of dry and wet sample of Sepia melanin by EPR response (see *Material and Methods*).

Sample	g-value	Linewidth, ΔB_{pp} (mT)	Resonance field, B_0 (mT)	Transverse relaxation time, T_2 (ns)
S_epr_dry	2.0034	0.62	336.90	66.4
S_epr_wet	2.0043	0.54	336.76	76.2

VSM analysis in ambient conditions

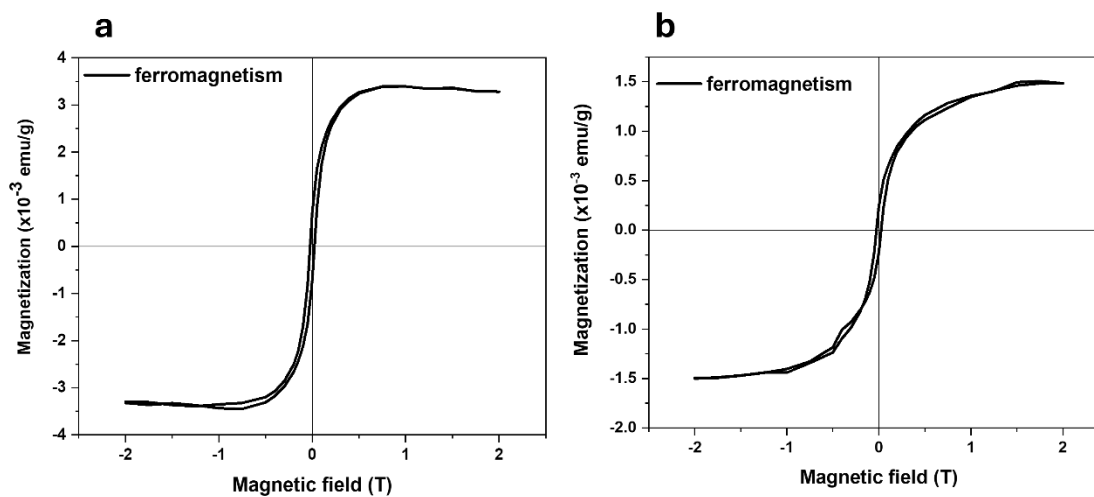


Fig. 2: M-H loop for (a) dry (S2_dry) and (b) wet (S2_wet) samples of Sepia melanin in ambient conditions ($1 \text{ emu/g} = 1 \text{ A.m}^2/\text{kg}$)

We ran VSM measurements on dry and wet samples of Sepia melanin in ambient conditions (see SI Table S2 i.e. S2_dry and S2_wet). We removed the contribution of the rod sample holder to get the contribution of the Sepia melanin only (Fig. S1 and S2) then we further removed the diamagnetic contribution (Fig. S1 and S2) from the total contribution to get the ferromagnetic contribution (Fig. 2 a and b). VSM measurements show weak ferromagnetic behavior (small



hysteresis) in both dry and wet samples, which might be attributed to the ordering of paramagnetic centers in the melanin.^{12, 41}

We observed a decrease in saturation magnetization (i.e. maximum magnetization reached when all magnetic moments in the material are aligned with the applied field) and remanent magnetization (i.e. residual magnetization left in the material after removing the external magnetic field) upon hydration, in agreement with previous EPR measurements on dry and wet samples.^{13, 35} Regarding the coercive field (i.e. magnetic field required to reduce the magnetization to zero after the material has been magnetized), it seems not to be affected by hydration. The values of M_s , M_r and H_c for dry and wet samples of Sepia melanin (Table 2) suggest that, in the dry state, the radicals are closer due to tighter molecular packing.¹³

We provided the comparison of magnetic parameters of different dry and wet samples in Table S1 for VSM measurements.

Table 2: Comparison of magnetic parameters of dry and wet samples of Sepia melanin (1 emu/g = 1 A.m²/kg).

Sample	M_s ($\times 10^{-3}$ emu/g)	M_r ($\times 10^{-3}$ emu/g)	H_c (mT)
S2_dry	3.6	0.64	23.6
S2_wet	1.5	0.26	26.1

Temperature-resolved VSM

We ran the temperature-resolved VSM studies for dry (see SI Table S2 i.e. S2_dry_P1) sample of Sepia melanin in the temperature range 150-360 K at steps of 70 K (Fig. S1) to investigate how temperature influences its magnetic behavior. We observed the decrease in M_s (Fig. 3a) with temperature whereas diamagnetism remains almost independent on the temperature. This behavior is typical of ferromagnetic systems: as temperature increases, thermal energy increases spin disorder. In Sepia melanin too, thermal agitation misaligns spin orientations, thus reducing the net magnetic moment.^{11, 35, 36} We also analyzed the remanent magnetization and coercivity with



temperature (Fig. 3 and Fig. 5), M_r and H_c decreases monotonously with temperature but even at 360 K, Sepia melanin shows the weak ferromagnetism with a coercivity of 23 mT (or 230 Oe). In the inset, we included the M-H loop in the range of magnetic field from -0.05 to 0.05 T.

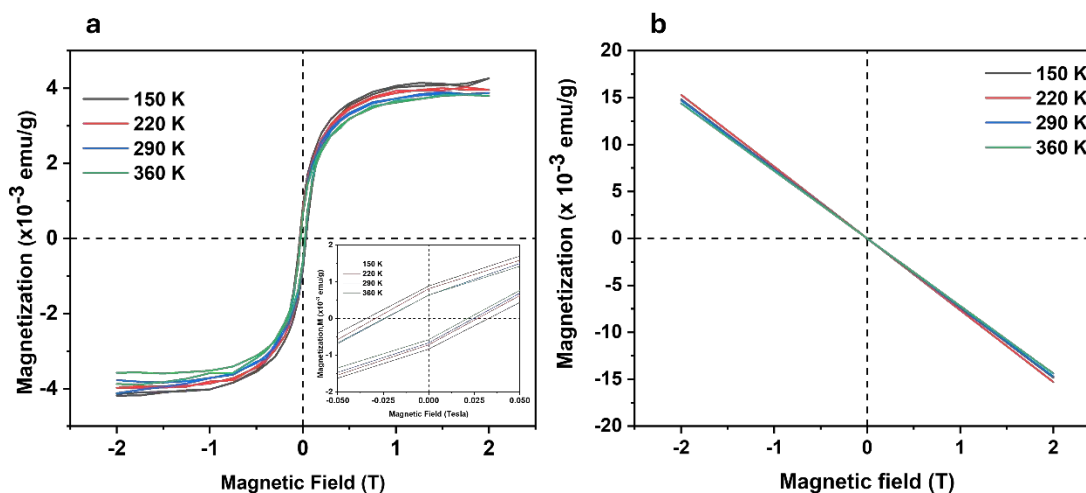


Fig. 3: Temperature dependent (a) M-H loop and (b) diamagnetism for dry (S2_dry_P1) sample of Sepia melanin ($1 \text{ emu/g} = 1 \text{ A.m}^2/\text{kg}$).

We also ran temperature-resolved VSM on wet (see SI Table S2 i.e. S2_wet_P1) samples of Sepia melanin in the same temperature range as dry one (Fig. S2). We observed the same behavior for wet and dry samples (Fig. 4a and b). Notably, the dry sample consistently exhibits higher magnetization across temperatures than the wet sample, reaffirming that hydration weakens magnetic interactions.^{13, 14} For the diamagnetic contribution from Sepia melanin, we plotted the susceptibility vs temperature (Fig. S3) for dry and wet sample and observed that susceptibility is almost temperature independent in both the cases. We calculated the value of susceptibility to be approximately $-7 \times 10^{-7} \text{ emu g}^{-1} \text{ Oe}^{-1}$ for both dry and wet samples (see SI, Fig. S3). A negative and temperature independent value of susceptibility is expected for diamagnetism. Please note that in the inset of Fig. 4a, we included the M-H loop in the range of magnetic field from -0.05 to 0.05 T.

The values of M_s , M_r and H_c with temperature for comparison are shown in Fig. 5 and Table S2.



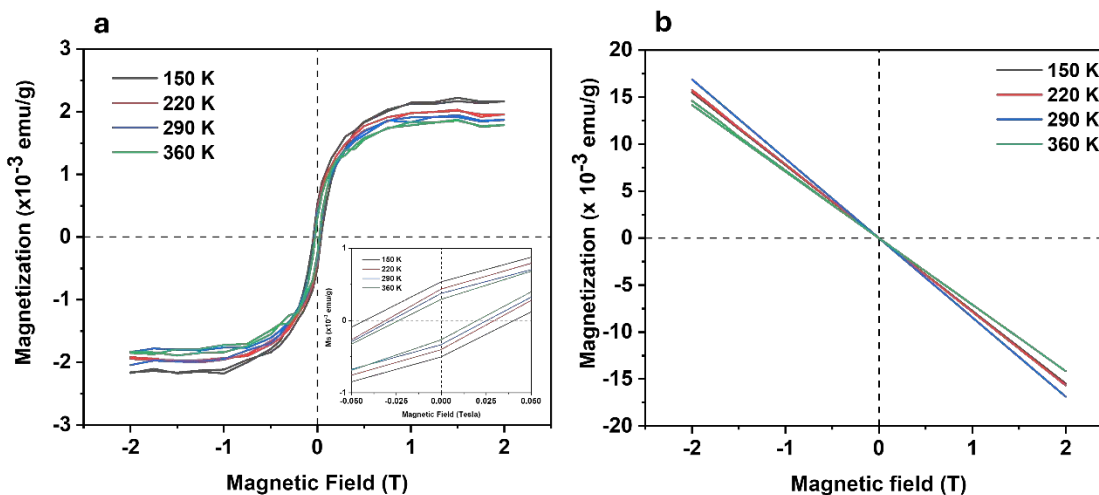


Fig. 4: Temperature dependent (a) M-H loop and (b) diamagnetism for wet (S2_wet_P1) sample of *Sepia melanin* ($1 \text{ emu/g} = 1 \text{ A.m}^2/\text{kg}$).

Fig. 5 represents the behavior of M_s , M_r and H_c with temperature for dry and wet samples of *Sepia melanin* (Table S2). All these factors, i.e. M_s , M_r and H_c , decreases monotonously with temperature but persist up to 360 K, where there is a small coercivity of $\sim 23 \text{ mT}$ (or 230 Oe) for both dry and wet samples. M_s and M_r are higher in the dry sample at each temperature as compared to dry sample, but H_c is higher in the wet sample.

Using a simple mean field model of the spontaneous magnetization of a ferromagnet as a function of temperature, we estimated a transition temperature of $\sim 550 \text{ K}$ for the dry sample and $\sim 420 \text{ K}$ for the wet sample (see Fig S4 in Supplementary Information). This further supports the assumption that the hydration weakens the ferromagnetic ordering.



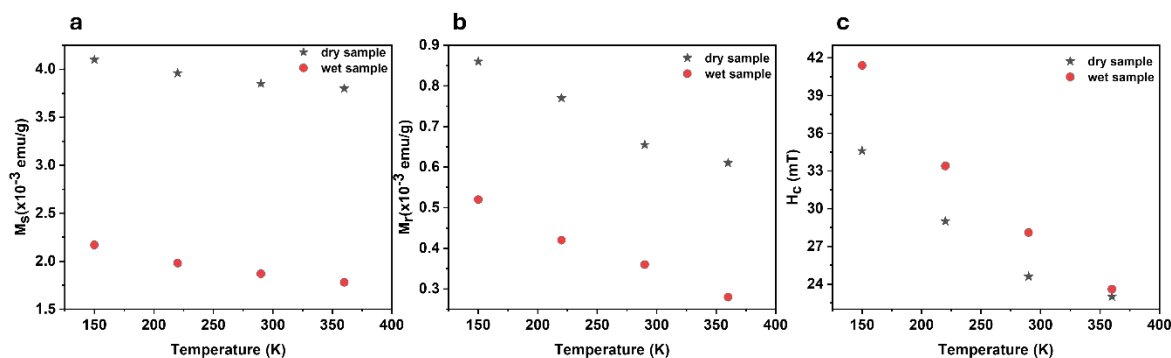


Fig. 5: Magnetic parameters as a function of temperature: (a) Saturation magnetization, M_s (b) Remanent magnetization, M_r and (c) Coercivity, H_c for dry (S2_dry_P1) and wet (S2_wet_P1) samples of Sepia melanin ($1 \text{ emu/g} = 1 \text{ A}\cdot\text{m}^2/\text{kg}$).

INAA

To further verify the presence of transition metals in the Sepia melanin, we ran INAA on the samples in order to determine the mass fractions of Cu, Fe, Co and Ni. The results of this analysis are presented in Table 3. The reported concentrations are provided with a confidence interval of 68% (one standard deviation) on the net photopeak statistic when the gamma-ray signal was above background. In the case of Ni, no clear photopeak was measured above the background signal and thus detection limits with a 95% confidence interval (two standard deviations) were given. Consequently, INAA revealed only 86.7 ppm of Fe in the bulk of the sample and much lower amounts of Cu, Ni and Co. This low concentration, coupled with the absence of Fe signals in XPS, suggests that iron is present only in trace amounts and do not contribute significantly to the observed magnetization. Furthermore, the measured M_s of $4.1 \times 10^{-3} \text{ emu/g}$ (dry) and $2.17 \times 10^{-3} \text{ emu/g}$ (wet) far exceeds the theoretical maximum of $4.72 \times 10^{-5} \text{ emu/g}$ attributable to the detected Fe content, reinforcing the idea that the magnetization cannot originate from metal impurities only. Although the measured magnetization values are small, several features support the presence of



ferromagnetism in Sepia melanin. First, the presence of a finite coercive field and remanent magnetization indicates hysteresis behavior that is not expected for purely paramagnetic materials. Furthermore, the highly non-linear magnetization response vs. the applied field at room temperature cannot be explained by a paramagnetic behavior originating from non-interacting magnetic moments. We evaluated the maximal expected contribution to the magnetisation of transition metals using concentrations obtained from INAA, which revealed trace concentrations of Fe (≈ 86 ppm) and even smaller amounts of Cu (≈ 19 ppm), Co (≈ 0.137 ppm), and Ni (< 4.4 ppm). The theoretical magnetization expected from the measured Fe content is approximately $\sim 10^{-5}$ emu/g (see Calculation S2 in Supplementary Information for further details), which is significantly lower than the experimentally observed magnetization ($\sim 10^{-3}$ emu/g), suggesting that the metal impurities detected do not account for the magnetic response. Instead, it is more plausible that the magnetization is intrinsically linked to the properties of melanin, particularly since the presence of stable semiquinone radicals is known to host unpaired electron spins. The observation of a clear hysteresis suggests that short-range, locally ordered spin interactions are present in these radicals, highlighting Sepia melanin as a truly organic ferromagnetic material.

Table 3: Concentration (in ppm) of Cu, Fe, Co and Ni in Sepia melanin powder as obtained through INAA.

Cu		Fe		Co		Ni	
Value	Uncert.	Value	Uncert.	Value	Uncert.	Value	Uncert.
19.3	1.3	86.7	12.3	0.137	0.037	<4.4	-

XPS Analysis



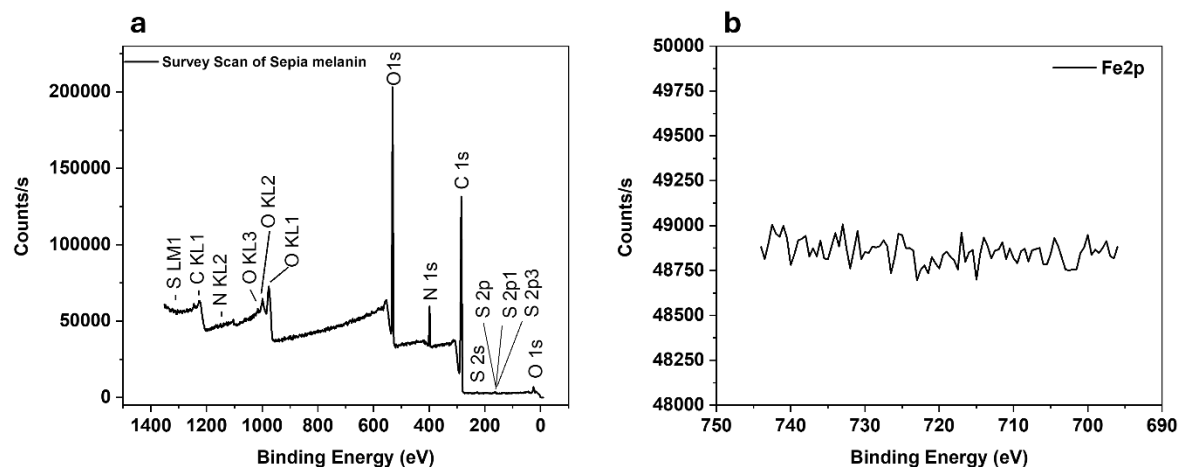


Fig. 6: XPS spectra of Sepia melanin (a) survey scan and (b) Fe2p.

To further verify that whether the magnetization observed in EPR and VSM measurements of Sepia melanin is not linked to the presence of metal ions, we conducted elemental analysis using XPS. The survey scan (Fig. 6a) revealed clear peaks corresponding to carbon (C 1s), nitrogen (N 1s), and oxygen (O 1s), consistent with the expected composition of Sepia melanin. No signals associated with transition metals were detected. To specifically investigate the presence of iron, a scan of the Fe 2p region (Fig. 6b) was performed, which showed no evidence of Fe 2p_{3/2} or Fe 2p_{1/2} peaks. This indicates that iron is not present at the surface of the sample, at least within the detection limits of XPS. The absence of detectable metal signals in the XPS spectra does not imply a complete absence of metals but rather indicates that their surface concentration is below the detection limit of XPS of about 1000 part per million (ppm).

Conclusion

This study provides a comprehensive investigation of the magnetic properties of Sepia melanin biopigment obtained from acid-treated edible cuttlefish using Electron Paramagnetic Resonance (EPR) and Vibrating Sample Magnetometry (VSM), in both dry and hydrated states, over a broad temperature range. EPR measurements reveal that hydration leads to a decrease in signal intensity,



a slight shift in the g -value and an increase of transverse relaxation time, suggesting that water molecules alter the local electronic environment and disrupt radical interactions. The VSM results suggest the presence of weak ferromagnetism in Sepia melanin, which might be arising from localized π -radical interactions and spin–spin exchange between CCR as proposed in literature. VSM measurements further show that hydration causes a reduction in M_s , M_r , and H_c . Furthermore, temperature-resolved VSM measurements (150–360 K) suggest weak ferromagnetism (persisting up to 360 K) for both dry and hydrated samples. A mean-field model of spontaneous magnetization of ferromagnet is used to estimate the transition temperatures of ~ 550 K and ~ 420 K for dry and wet samples of Sepia melanin, respectively. The results of INAA revealed that the concentration of metals is in trace amount thus suggesting that the measured magnetic response is dominated by intrinsic radical centers. These advances reveal the potential of Sepia melanin as a radical-based organic magnetic material and offer a mechanistic link between hydration, radical dynamics, and magnetic ordering. Overall, the findings emphasize the intrinsic and tunable magnetic characteristics of Sepia melanin, governed by its radical content, π – π interactions, and environmental factors. We plan to systematically investigate hydration-dependent electronic conductivity (using both contact and contactless methods) to explore its correlation with the magnetic parameters.

Author contributions

Conceptualization: C. Santato, S. Khaleel; data curation: C. Santato, S. Khaleel, C. Lacroix, D. Hall, D. Menard; investigation: S. Khaleel, C. Lacroix, D. Hall; methodology: S. Khaleel, C. Lacroix, D. Menard, C. Santato; funding acquisition: C. Santato, M. Cavarroc; resources: C.



Santato, D. menard, D. Hall; supervision: C. Santato, D. Menard, M. Cavorroc; writing original draft: S. Khaleel; writing, reviewing and editing: all authors.

Conflicts of interest

The authors declare no conflicts of interest.

Data availability

All supporting data are available in the Supplementary Information.

Acknowledgements

C.S. is grateful to NSERC (D.G. RGPIN-2022-04640) and the CRC (Canada Research Chair in Sustainable Organic Electronics, 950-232719), for financial support. The authors gratefully acknowledge Prof. Daria C. Boffito for access to the EPR instrumentation and Nila Davari for her valuable assistance during the EPR experiments. The authors also acknowledge Dr. Josianne Lefebvre for assistance with XPS data acquisition.

- (1) Baumgartner, M.; Coppola, M. E.; Sariciftci, N. S.; Glowacki, E. D.; Bauer, S.; Irimia-Vladu, M. Emerging “green” materials and technologies for electronics. *Green Materials for Electronics* **2017**, *101* (1).
- (2) Birajdar, M. S.; Joo, H.; Koh, W.-G.; Park, H. Natural bio-based monomers for biomedical applications: a review. *Biomaterials Research* **2021**, *25* (1), 8.
- (3) Sun, D.; Ehrenfreund, E.; Vardeny, Z. V. The first decade of organic spintronics research. *Chemical communications* **2014**, *50* (15), 1781-1793.
- (4) Miller, J. S. Molecular/organic magnets—potential applications. *Advanced Materials* **1994**, *6* (4), 322-324.
- (5) Miller, J. S.; Epstein, A. J. Molecule-based magnets—an overview. *Mrs Bulletin* **2000**, *25* (11), 21-30.
- (6) White, R. Opportunities in magnetic materials. *Science* **1985**, *229* (4708), 11-15.
- (7) Blundell, S. J.; Pratt, F. L. Organic and molecular magnets. *Journal of Physics: Condensed Matter* **2004**, *16* (24), R771.
- (8) Miller, J. S. Organic-and molecule-based magnets. *Materials Today* **2014**, *17* (5), 224-235.
- (9) McConnell, H. M. Ferromagnetism in solid free radicals. *The Journal of Chemical Physics* **1963**, *39* (7), 1910-1910.
- (10) Tamura, M.; Nakazawa, Y.; Shiomi, D.; Nozawa, K.; Hosokoshi, Y.; Ishikawa, M.; Takahashi, M.; Kinoshita, M. Bulk ferromagnetism in the β -phase crystal of the p-nitrophenyl nitronyl nitroxide radical. *Chemical Physics Letters* **1991**, *186* (4-5), 401-404.



- (11) Mahmood, J.; Park, J.; Shin, D.; Choi, H.-J.; Seo, J.-M.; Yoo, J.-W.; Baek, J.-B. Organic ferromagnetism: trapping spins in the glassy state of an organic network structure. *Chem* **2018**, *4* (10), 2357-2369.
- (12) Al Khatib, M.; Costa, J.; Baratto, M. C.; Basosi, R.; Pogni, R. Paramagnetism and relaxation dynamics in melanin biomaterials. *The Journal of Physical Chemistry B* **2020**, *124* (11), 2110-2115.
- (13) Mostert, A. B.; Hanson, G. R.; Sarna, T.; Gentle, I. R.; Powell, B. J.; Meredith, P. Hydration-controlled X-band EPR spectroscopy: A tool for unravelling the complexities of the solid-state free radical in eumelanin. *The Journal of Physical Chemistry B* **2013**, *117* (17), 4965-4972.
- (14) Paulin, J. V.; Graeff, C. F.; Mostert, A. B. Decoding eumelanin's spin label signature: a comprehensive EPR analysis. *Materials Advances* **2024**, *5* (4), 1395-1419.
- (15) Camus, A.; Choe, S.; Bour-Cardinal, C.; Isasmendi, J.; Cho, Y.; Kim, Y.; Irimia, C. V.; Yumusak, C.; Irimia-Vladu, M.; Rho, D. Electrical response and biodegradation of Sepia melanin-shellac films printed on paper. *Communications Materials* **2024**, *5* (1), 173.
- (16) d'Ischia, M.; Napolitano, A.; Pezzella, A.; Meredith, P.; Sarna, T. Chemical and structural diversity in eumelanins: unexplored bio-optoelectronic materials. *Angewandte Chemie International Edition* **2009**, *48* (22), 3914-3921.
- (17) Reali, M.; Gouda, A.; Bellemare, J.; Ménard, D.; Nunzi, J.-M.; Soavi, F.; Santato, C. Electronic transport in the biopigment sepia melanin. *ACS Applied Bio Materials* **2020**, *3* (8), 5244-5252.
- (18) Wünsche, J.; Deng, Y.; Kumar, P.; Di Mauro, E.; Josberger, E.; Sayago, J.; Pezzella, A.; Soavi, F.; Cicoira, F.; Rolandi, M. Protonic and electronic transport in hydrated thin films of the pigment eumelanin. *Chemistry of Materials* **2015**, *27* (2), 436-442.
- (19) Cheng, J.; MOSS, S. C.; EISNER, M. X-ray characterization of melanins—II. *Pigment Cell Research* **1994**, *7* (4), 263-273.
- (20) Niyonkuru, D.; Camus, A.; Reali, M.; Gao, Z.; Shadrack, D. M.; Butyaev, O.; Surtchev, M.; Santato, C. A nanoscale study of the structure and electrical response of Sepia eumelanin. *Nanoscale Advances* **2023**, *5* (19), 5295-5300.
- (21) Blois, M.; Zahlan, A.; Maling, J. Electron spin resonance studies on melanin. *Biophysical Journal* **1964**, *4* (6), 471-490.
- (22) Blois, M. S. The melanins: their synthesis and structure. In *Photochemical and Photobiological Reviews: Volume 3*, Springer, 1978; pp 115-134.
- (23) Felix, C.; Hyde, J.; Sarna, T.; Sealy, R. Interactions of melanin with metal ions. Electron spin resonance evidence for chelate complexes of metal ions with free radicals. *Journal of the American Chemical Society* **1978**, *100* (12), 3922-3926.
- (24) Meredith, P.; Sarna, T. The physical and chemical properties of eumelanin. *Pigment cell research* **2006**, *19* (6), 572-594.
- (25) Mostert, A. B.; Powell, B. J.; Pratt, F. L.; Hanson, G. R.; Sarna, T.; Gentle, I. R.; Meredith, P. Role of semiconductivity and ion transport in the electrical conduction of melanin. *Proceedings of the National Academy of Sciences* **2012**, *109* (23), 8943-8947.
- (26) Paulin, J.; Batagin-Neto, A.; Meredith, P.; Graeff, C.; Mostert, A. Shedding light on the free radical nature of sulfonated melanins. *The Journal of Physical Chemistry B* **2020**, *124* (46), 10365-10373.



- (27) Paulin, J. o. V.; Batagin-Neto, A.; Graeff, C. F. Identification of common resonant lines in the EPR spectra of melanins. *The Journal of Physical Chemistry B* **2019**, *123* (6), 1248-1255.
- (28) D'Amora, U.; Soriente, A.; Ronca, A.; Scialla, S.; Perrella, M.; Manini, P.; Phua, J. W.; Ottenheim, C.; Di Girolamo, R.; Pezzella, A. Eumelanin from the black soldier fly as sustainable biomaterial: characterisation and functional benefits in tissue-engineered composite scaffolds. *Biomedicines* **2022**, *10* (11), 2945.
- (29) Sever, R. J.; Cope, F. W.; Polis, B. D. Generation by visible light of labile free radicals in the melanin granules of the eye. *Science* **1962**, *137* (3524), 128-129.
- (30) Felix, C.; Hyde, J.; Sarna, T.; Sealy, R. Melanin photoreactions in aerated media: electron spin resonance evidence for production of superoxide and hydrogen peroxide. *Biochemical and biophysical research communications* **1978**, *84* (2), 335-341.
- (31) Arnaud, R.; Perbet, G.; Deflandre, A.; Lang, G. Electron spin resonance of melanin from hair. Effects of temperature, pH and light irradiation. *Photochemistry and photobiology* **1983**, *38* (2), 161-168.
- (32) Camus, A.; Reali, M.; Rozel, M.; Zhuldybina, M.; Soavi, F.; Santato, C. High conductivity Sepia melanin ink films for environmentally benign printed electronics. *Proceedings of the National Academy of Sciences* **2022**, *119* (32), e2200058119.
- (33) Foner, S. Versatile and sensitive vibrating-sample magnetometer. *Review of Scientific Instruments* **1959**, *30* (7), 548-557.
- (34) Foner, S. The vibrating sample magnetometer: Experiences of a volunteer. *Journal of applied physics* **1996**, *79* (8), 4740-4745.
- (35) Madkhali, N.; All, N. A.; Algessair, S.; Aodah, S. H. Magnetic and optical investigation of Eumelanin-ZnO as organic-non-organic nanocomposite. *Optik* **2021**, *225*, 165772.
- (36) Khouqeer, G.; Alghrably, M.; Madkhali, N.; Dhahri, M.; Jaremko, M.; Emwas, A. H. Preparation and characterization of natural melanin and its nanocomposite formed by copper doping. *Nano Select* **2022**, *3* (12), 1598-1608.
- (37) Sarzanini, C.; Mentasti, E.; Abollino, O.; Fasano, M.; Aime, S. Metal ion content in Sepia officinalis melanin. *Marine chemistry* **1992**, *39* (4), 243-250.
- (38) Khaleel, S.; Gao, Z.; Camus, A.; Isasmendi Ramirez, O. J.; Cavarroc-Weimer, M.; Santato, C. Melanin granules extracted from Sepia ink: A nanoscale study of charge carrier transport. *Journal of Physics: Materials* **2025**, *8* (3), 035002.
- (39) Hunter, C. A.; Sanders, J. K. The nature of pi.-pi. interactions. *Journal of the American Chemical Society* **1990**, *112* (14), 5525-5534.
- (40) Abramov, P.; Ivankov, O.; Mostert, A.; Motovilov, K. Signatures of pancake bonding in hydrated eumelanin. *Physical Chemistry Chemical Physics* **2023**, *25* (24), 16212-16216.
- (41) Bolzoni, F.; Giraudo, S.; Lopiano, L.; Bergamasco, B.; Fasano, M.; Crippa, P. R. Magnetic investigations of human mesencephalic neuromelanin. *Biochimica et Biophysica Acta (BBA)-Molecular Basis of Disease* **2002**, *1586* (2), 210-218.



Data availability

All supporting data are available in the Supplementary Information.

